

A spectroscopic study on Calf thymus DNA binding properties of nickel (II) complex with imidazole derivatives of 1,10-phenanthroline ligand

Alireza Aminikhoushani^a, Nasrin Sohrabi^{a,*}, Nahid Rasouli^{a,*}, Mahboube Eslami Moghadam^b

^aDepartment of Chemistry, Payame Noor University, P.O. BOX 19395-3697 Tehran, Iran

^bChemistry & Chemical Engineering Research Center of Iran, Tehran, Iran.

Received: 7 April 2016, Accepted: 3 October 2016, Published: 3 October 2016

Abstract

In this study, a nickel (II) complex with 1,10-phenanthroline based ligand, $[\text{Ni}(\text{FIP})_2](\text{OAC})_2$ (1) with FIP = 2-(Furan-2-yl)-1H-Imidazole[4,5-f][1,10]phenanthroline as ligand was synthesized and characterized by spectroscopic methods and elemental analysis. The interaction of $[\text{Ni}(\text{FIP})_2](\text{OAC})_2$ (1) with calf-thymus DNA (ct-DNA) was studied by UV-Vis absorption, fluorescence spectroscopies and viscosity measurements in 20 mM Tris/HCl buffer solution, pH 7.0 at 25 °C. The complex (1) interacts with ct-DNA with an intrinsic binding constant of $1.11 \times 10^5 \text{ M}^{-1}$. Furthermore, the thermodynamic studies suggested that the interaction processes were endothermic disfavored ($\Delta H > 0$) and entropy favored ($\Delta S > 0$). The viscosity studies showed no considerable increasing changes in the viscosity of ct-DNA with increasing of the complex (1) concentration. Therefore, the $[\text{Ni}(\text{FIP})_2](\text{OAC})_2$ complex bind to ct-DNA *via* hydrophobic interaction as the main forces acting during the binding processes and the mode of binding is groove binding which was illustrated by hyperchromism in the UV-Vis absorption band of $[\text{Ni}(\text{FIP})_2](\text{OAC})_2$ (1) with addition of ct-DNA and the decreasing of ethidium bromide (EB)-ct-DNA complex fluorescence in the presence of different concentrations of $[\text{Ni}(\text{FIP})_2](\text{OAC})_2$ complex and the unchanged viscosity of ct-DNA.

Keywords: Nickel complex; imidazole derivatives; DNA binding.

Introduction

Research on metal complexes that are used as anti-cancer drugs is of special importance [1,2]. So, studies on the interaction of metal complexes with nucleic acid is of great importance because of their application in the synthesis of novel drugs with effective therapeutic effects [3,4]. In general, metal complexes which can interact with DNA by covalent interaction

include the coordination of the nitrogenous base or the phosphate group of the nucleic acid to the central metal ion or non-covalent interaction which include intercalation, groove binding or external electrostatic binding [5]. Interaction of metal complexes with nucleic acid can inhibit DNA repair by interfering with enzymes or proteins involved in DNA replication or DNA repair [6]. Among the metal

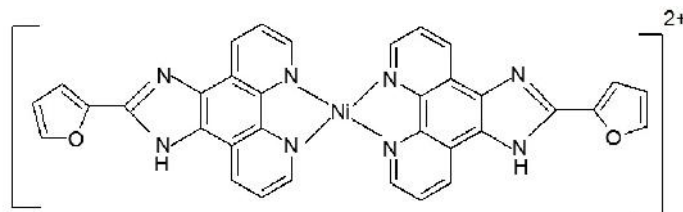
*Corresponding author: Nahid Rasouli

Tel: +98 (31) 32608028, Fax: +98 (31) 32608028

E-mail: n.rasouli@pnu.ac.ir, n.rasouli55@yahoo.com

complexes, nickel complexes have received much interest due to their interesting binding properties and cleavage reactivity with nucleic acid [7,8]. On the other hand, 1,10-phenanthroline and its derivatives were usually served as a very important class of ligands, which lead to efficient catalysis in cross coupling reaction of aliphatic alcohols and aryl halides [9], antimicrobial activity [10], efficient DNA-binding and DNA cleavage [11]. So far, special attentions have been paid to transition metal complexes with imidazole [4,5-f][1,10] phenanthroline derivative ligand [12,13]. However, there have been few studies on nickel (II) complexes with imidazole

derivatives of 1,10-phenanthroline and its interaction with ct-DNA. Recently, we have reported the binding of human serum albumin with palladium (II) complexes containing of imidazole derivatives of 1,10-phenanthroline ligand [14]. Herein, we report the interaction nickel (II) complex with 1,10-phenanthroline-based ligand, $[\text{Ni}(\text{FIP})_2](\text{OAC})_2$ (**1**) (Scheme 1) and ct-DNA to study the behavior of this class of compounds with ct-DNA. So, several techniques were used for investigation of interactions between $[\text{Ni}(\text{FIP})_2](\text{OAC})_2$ complex and ct-DNA.



Scheme 1. The chemical structure of $[\text{Ni}(\text{FIP})_2](\text{OAC})_2$ complex

Experimental

Materials and preparation

Calf thymus DNA was purchased from Sigma Chemical Co. All of the other chemicals were in analytical grades and purchased from Merck and Sigma. The water soluble cationic complex (**1**) was prepared and purified according to literature method. This complex was characterized by IR and UV-Vis spectroscopies and elemental analysis. All experiments were run in 20 mM Tris/HCl buffer solution at pH= 7.0 at 25 °C. Concentrations expressed in moles of base pairs per liter were obtained using $=1.32 \times 10^4 \text{ L.mol}^{-1}.\text{cm}^{-1}$ at the absorption maximum of 260 nm. Infrared spectra were recorded on a FT-IR Nicolet-IR 100 spectrometer using KBr pellets.

Elemental analysis of the complex (**1**) was performed by CHN Rapid Heraeus elemental analyzer. The pH values were controlled using a Metrohm-691 pH-meter.

Optical Absorption

The absorbance measurements were carried out using a Jenway UV-6800 recording double beam spectrophotometer operating from 200 to 700 nm in 1.0 cm quartz cells. The absorbance titrations were performed at a fixed concentration of the complex (**1**) ($2 \times 10^{-5} \text{ M}$) and varying the concentration of ct-DNA (0 - $5.36 \times 10^{-5} \text{ M}$).

Fluorescence Spectroscopy

All fluorescence measurements were carried out with a Hitachi MPF-4 spectrofluorimeter by keeping the

concentration of complex (1) constant while varying the ct-DNA concentration from 0 to 0.749, 1.42, 2.02, 2.57, 3.93 and 4.67 μM .

Viscosity Measurements

The viscosity of ct-DNA solution was measured at 25 ± 0.1 °C using an ostwald viscometer. Typically, 20 mM Tris/HCl buffer solution, pH 7 was transferred to the viscometer to obtain the reading of flow time. For determination of solution viscosity, 10 mL of buffered solution of ct-DNA (1.26×10^{-5} M) was taken to the viscometer and a flow time reading was obtained. An appropriate amount of complex (1) was then added to the viscometer to give a certain R ($R = [\text{Complex (1)}]/[\text{ct-DNA}]$) value while keeping the ct-DNA concentration constant and the flow time was read. The obtained data were presented as relative viscosity, $(\eta/\eta_0)^{1/3}$ versus R, where η is the reduced specific viscosity of ct-DNA in the presence of complex (1) and η_0 is the reduced specific viscosity of ct-DNA alone.

Synthesis of 2-(Furan-2-yl)-1H-Imidazole [4,5-f][1,10]phenanthroline (FIP)

The 2-(Furan-2-yl)-1H-Imidazole [4,5-f][1,10] phenanthroline (FIP) as ligand was synthesized according to the literature method [14]. The ligand as a brown solid was dried at 60 °C in an oven. Yield: % 85. FT-IR (KBr), (cm^{-1}): 3377 ($\nu_{\text{N-H}}$), 3075 ($\nu_{\text{C-H}}$), 1564 ($\nu_{\text{C=N}}$), 1425 ($\nu_{\text{C=C}}$), 1387, 1173, 1063, 1012, 943 ($\nu_{\text{C-H}}$), $^1\text{H-NMR}$ (400 MHz, DMSO- d_6): 6.76-6.79 (m, 1H), 7.25(d, 1H, $J=3$ Hz), 7.7-7.8 (m, 2H), 7.99 (d, 1H, $J=1.2$ Hz), 8.9 (d, 2H, $J=7.8$ Hz), 9.02 (d, 2H, $J=1.8$ Hz), 13.9 (br s, 1H, NH), Mp = 195-198 °C, UV-vis (ethanol): $\lambda_{\text{max}} = 317$ nm ($\epsilon = 13.8 \times 10^3 \text{ M}^{-1}\text{cm}^{-1}$).

Synthesis of $[\text{Ni}(\text{FIP})_2](\text{OAC})_2$ complex

A methanolic solution (10 mL) of the $\text{Ni}(\text{OAC})_2 \cdot 4\text{H}_2\text{O}$ (0.1 mmol) was added to a solution of FIP ligand (0.2 mmol) in methanol. The reaction mixture was refluxed for 2 h. The mixture was cooled to room temperature, the resulting brown solid was filtered, washed with ethanol and recrystallized in ethanol. The product was dried at 60°C in a vacuum oven. Yield: % 77. Analytical Calculated for $\text{NiC}_{29}\text{H}_{18}\text{N}_8\text{O}_7$: C, 61.10; H, 4.30; N, 14.24. Analytical found: C, 60.45; H, 4.61; N, 13.87. FT-IR (KBr), (cm^{-1}): 3416 ($\nu_{\text{O-H}}$), 3046 ($\nu_{\text{N-H}}$), 1604, 1574, 1550, 1522 ($\nu_{\text{C=N}}$), 436 ($\nu_{\text{M-L}}$).

Results and discussion

DNA Binding: Electronic absorption spectroscopy

The electronic absorption spectroscopy is one of the useful techniques in DNA-binding studies [15]. Hypochromic and hyperchromic effects are the spectra features of ct-DNA concerning changes in its double helical structure. The Hypochromism phenomena happens due to the intercalative mode involving strong stacking interaction between an aromatic chromophore and the base pairs of DNA. The hyperchromic effect related to electrostatic binding [16] or to partial uncoiling of the helix structure of DNA exposing more bases of the DNA [17]. The absorption spectrum of the $[\text{Ni}(\text{FIP})_2](\text{OAC})_2$ complex shows an inter-ligand charge transfer bands at 229 nm and the metal to ligand charge transfer band (MLCT) at 283 nm (Figure 1) [14].

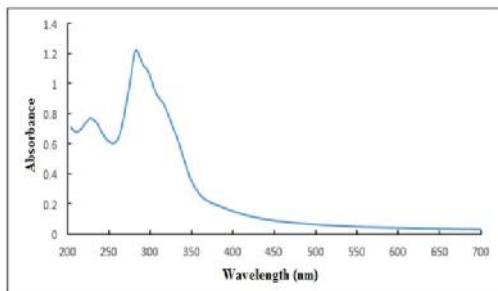


Figure 1. UV-Vis spectrum of $[\text{Ni}(\text{FIP})_2](\text{OAC})_2$ complex

The absorption intensity of the complex (**1**) in 20 mM Tris/HCl buffer solution, pH 7 and at 25 °C increased (hyperchromism) after the addition of ct-DNA, which indicated the interactions between ct-DNA and the complex (**1**) (Figure 2).

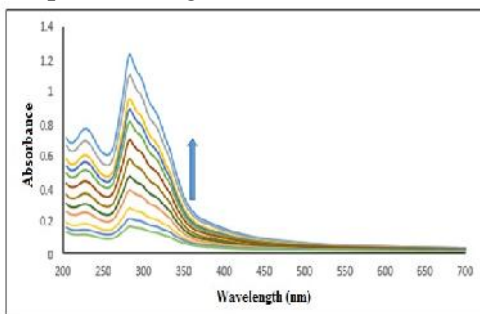


Figure 2. Absorption spectra of $[\text{Ni}(\text{FIP})_2](\text{OAC})_2$ (2×10^{-5} M) upon titration with solution of ct-DNA in 20 mM Tris/HCl buffer solution, pH 7 and at 25 °C

The complex (**1**) can bind to double strand DNA in different binding modes on the basis of the structure and type of the ligand. As DNA double helix possesses many hydrogen binding sites which are accessible in the minor and major grooves, it is likely that the $-\text{NH}$ -group of the complex (**1**) forms hydrogen bonds with DNA, which may contribute to the hyperchromism observed in the absorption spectra [18]. Also, the hyperchromic effect may be due to the electrostatic interaction between positively charged complex (**1**) and the negatively charged phosphate backbone at the periphery of the double helix DNA [19]. In order to

quantitatively compare the binding strength of $[\text{Ni}(\text{FIP})_2](\text{OAC})_2$, the intrinsic binding constant was determined according to this Eq. (1) [20]:

$$\frac{[\text{DNA}]}{(\epsilon_a - \epsilon_f)} = \frac{[\text{DNA}]}{(\epsilon_b - \epsilon_f)} + \frac{1}{K_b} \quad (1)$$

Where $[\text{DNA}]$ was the concentration of DNA, ϵ_a , ϵ_f and ϵ_b corresponded to the apparent extinction coefficient, the extinction coefficient of the free compound and its fully DNA-bound combination, respectively. In the plots of $[\text{DNA}]/(\epsilon_a - \epsilon_f)$ versus $[\text{DNA}]$, K_b was given by the ratio of the slope to intercept (Figure 3). The apparent binding constant of $[\text{Ni}(\text{FIP})_2](\text{OAC})_2$ complex was calculated to be $(1.11 \pm 0.01) \times 10^5 \text{ M}^{-1}$.

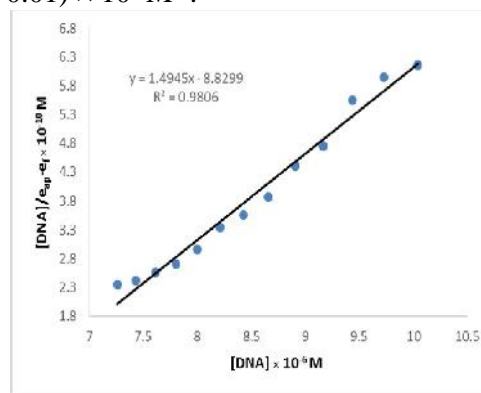


Figure 3. The plot of $[\text{ct-DNA}]/(\epsilon_{\text{app}} - \epsilon_f)$ versus $[\text{ct-DNA}]$

Moreover, the K_b value obtained was lower than that of classical intercalators [21-23] whose binding constants are on the order of 10^6 - 10^7 . Comparing the intrinsic binding constant of the complex (**1**) with those of known DNA groove binders we can deduce that this complex binds to ct-DNA *via* groove binding mode [24, 25].

Displacement studies

Fluorescence quenching which refers to any process is a decrease of the fluorescence intensity from a fluorophore due to a different molecular interaction. It is well known that the fluorescence intensity of DNA

itself is very weak and no fluorescence was observed for $[\text{Ni}(\text{FIP})_2](\text{OAC})_2$ complex. Therefore, use of its fluorescence emission properties to monitor the interaction of this complex with DNA is not possible. Ethidium bromide (EB) displays a dramatic enhancement of DNA fluorescence efficiency when intercalated into DNA [26]. When a second ligand which competed for the DNA binding sites was added, fluorescence quenching was observed [27]. Therefore, to investigate the extent of fluorescence quenching of EB binding to ct-DNA is used to determine the extent of binding between the second molecule and ct-DNA. The fluorescent emission of EB ($6.38 \times 10^{-5} \text{M}$) bound to ct-DNA in the presence of the increasing amounts of the complex (1) concentrations is shown in Fig. 4 which clearly shows a decrease in the fluorescence intensity of the EB-ct-DNA solution on addition of the complex (1), which indicating the replacement or electron transfer of EB by the complex (1) and decreasing the binding constant of EB to ct-DNA [28,29].

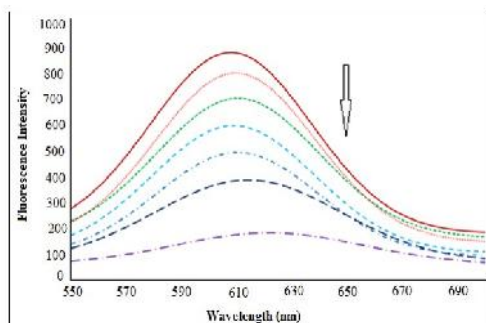


Figure 4. Emission spectra of the EB-ct-DNA complex in the presence of the increasing amounts of $[\text{Ni}(\text{FIP})_2](\text{OAC})_2$ complex in DNA/EB in 20 mM Tris/HCl buffer solution, pH 7 and at 25 °C

Fluorescence quenching efficiency is measured quantitatively with the Stern-Volmer equation (Eq.2).

$$F_0/F = 1 + K_{SV} [Q]$$

Where F_0 and F represent the emission intensity in the absence and presence of quencher, respectively, K_{SV} is a linear Stern–Vollmer quenching constant and $[Q]$ is the quencher concentration. K_{SV} obtained was 0.4213 M^{-1} . The Stern–Vollmer quenching plots from the fluorescence titration data are shown in Figure 5 and K_{SV} obtained was 0.4213 M^{-1} . The linear Stern-Volmer plot indicating that only one type of quenching process occurs.

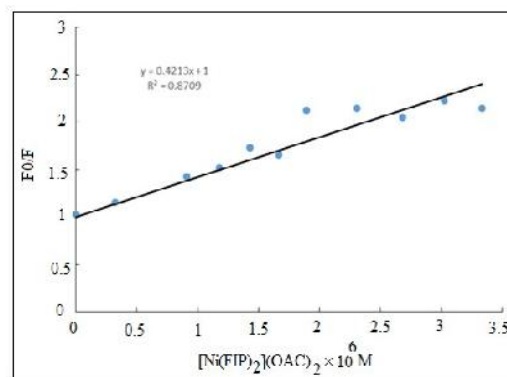


Figure 5. Plots of F_0/F versus the concentration of $[\text{Ni}(\text{FIP})_2](\text{OAC})_2$ complex for the binding of $[\text{Ni}(\text{FIP})_2](\text{OAC})_2$ with ct-DNA at room temperature

Thermodynamic Studies

In order to have a better understanding of thermodynamics of the reaction between $[\text{Ni}(\text{FIP})_2](\text{OAC})_2$ complex and ct-DNA, it is useful to determine the contributions of thermodynamic parameters. From the viewpoint of thermodynamics, $H > 0$ and $S > 0$ reflect hydrophobic interaction; $H < 0$ and $S > 0$ imply an electrostatic force; $H < 0$ and $S < 0$ suggest the van der Waals force and hydrogen bond. If the temperature does not vary significantly, the enthalpy change can be regarded as

a constant. Based on the binding constant at different temperatures, the free energy change can be estimated by the following equations (Eq.3 & Eq.4):

$$\ln K_b = -\frac{H^\circ}{RT} + \frac{S^\circ}{R} \quad (3)$$

$$G^\circ = H^\circ - T S^\circ = -RT \ln K_b \quad (4)$$

Where K_b is the binding constant at the corresponding temperature and R is the gas constant. The plot of $\ln K_b$ versus $1/T$ allows the determination of H° and S° (Figure 6).

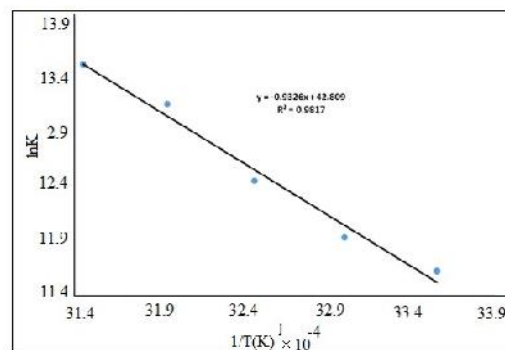


Figure 6. The van't Hoff plot $[\text{Ni}(\text{FIP})_2](\text{OAC})_2$ binding to ct-DNA

The thermodynamic parameters for the interaction of the complex (1) with ct-DNA are summarized in Table 1.

Table 1. Thermodynamic parameters for the interaction of $[\text{Ni}(\text{FIP})_2](\text{OAC})_2$ with ct-DNA in 20 mM Tris/HCl buffer solution, pH 7.0 at various temperatures

T/K	K_b	$\ln K_b$	G°	H°	S°
298	111000	11.61729	-28768.8	77499/89	356.6064
303	150000	11.91839	-30009.7	77499/89	354.817
308	250000	12.42922	-31812.3	77499/89	354.9098
313	500000	13.12236	-34131.7	77499/89	356.6503
318	714000	13.47864	-35618.4	77499/89	355.7178

It can be seen that the negative sign for G° values revealed the interaction process is spontaneous. By applying this analysis to the binding system of the complex (1) and ct-DNA, we determined that $H > 0$ and $S > 0$. Therefore, hydrophobic interactions are the main forces acting during the binding of complex (1) to ct-DNA and the mode of binding is hydrophobic binding. Consequently, the release of water molecules or counter ions results in positive enthalpy and entropy values in complex (1)-ct-DNA interactions.

Viscosity Study

Optical photophysical measurements provide necessary but not sufficient evidence for a binding model. Measurements of ct-DNA viscosity provide a critical test in the absence of crystallographic structural data. A feature of the intercalative binding mode was the lengthening of the double helix DNA by separation of DNA base pairs, which leading to a significant increase in ct-DNA viscosity. In contrast, there was little effect on the viscosity of the ct-DNA if groove or electrostatic binding occurred in the

binding process [31,32]. In order to explore the binding mode of $[\text{Ni}(\text{FIP})_2](\text{OAC})_2$ complex, viscosity measurements were carried out on ct-DNA by varying the concentration of the complex (1). The values of relative specific viscosity $(\eta_{sp}/c)^{1/3}$ vs. R ($R = [\text{Ni}(\text{FIP})_2](\text{OAC})_2 / [\text{ct-DNA}]$) (where η_{sp} and c are the specific viscosity of ct-DNA in the absence and in the presence of the $[\text{Ni}(\text{FIP})_2](\text{OAC})_2$ complex, respectively) were plotted (Figure 7).

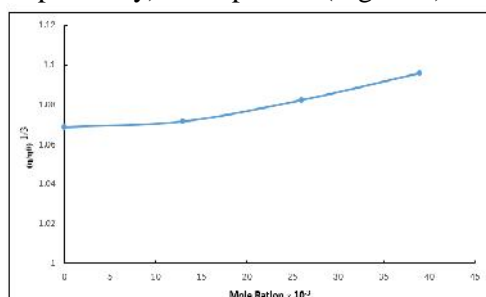


Figure 7. Relative viscosity of ct-DNA (1.35×10^{-5} M) in the presence of increasing amounts of $[\text{Ni}(\text{FIP})_2](\text{OAC})_2$ at stoichiometric ratios $R = [\text{Ni}(\text{FIP})_2](\text{OAC})_2 / [\text{ct-DNA}] = 0.0-0.039$, plotted as $(\eta_{sp}/c)^{1/3}$ vs. R. Measurements were done in 20 mM Tris/HCl buffer, pH 7 and at 25 °C

The relative viscosity of ct-DNA shows small rises with increase in the concentration of the complex (1), which is not similar to the classical intercalators such as ethidium bromide [33-35]. The viscosity results show that complex (1) bind to ct-DNA by groove or electrostatic binding mode and these results are in agreement with optical absorption experiments.

Conclusion

In summary, we have studied the binding mode of ct-DNA with a nickel (II) complex, $[\text{Ni}(\text{FIP})_2](\text{OAC})_2$ containing imidazole derivatives of 1,10-phenanthroline ligand. The results of UV-Vis and fluorescence spectroscopies suggest that the complex (1) interact with ct-DNA via

hydrophobic mode. The thermodynamic parameters ($\Delta H^\circ > 0$ and $\Delta S^\circ > 0$) showed that the increasing entropy caused by interaction with the complex arises from the hydrophobic interaction. The negative ΔG° values for interaction of ct-DNA with the complex (1) indicate spontaneity of the complex formation. The results showed that the relative viscosity of ct-DNA unchanged which is consistent with ct-DNA groove or electrostatic binding mode.

Acknowledgements

We are grateful to the Research Council of Payame Noor University for their financial supports.

References

- [1] J.B. Chaires, *Biopolymers.*, **1998**, *44*, 201-215.
- [2] A.M. Pyle, J.P. Rehman, R. Meshoyrer, C.V. Kumar, N. J.Turro, J.K. Barton, *J.Am.Chem.Soc.*, **1989**, *111*, 3051-3058.
- [3] K. Naing, M. Takahashi, M. Taniguchi, A. Yamagishi, *Bull.Chem. Soc. Jpn.*, **1994**, *67*, 2424-2429.
- [4] K.E. Erkkila, D.T. Odom, J.K. Barton, *Chem. Rev.*, **1999**, *99*, 2777-2796.
- [5] N. Shahabadi, L. Heidari, *Spectrochim Acta A: Mol Biomol Spec.*, **2014**, *128*, 377-385.
- [6] D.M. Kong, J. Wang, L.N. Zhu, Y.W. Jin, X.Z. Li, X. H. Shen, H.F. Mi, *J. Inorg. Biochem.*, **2008**, *102*, 824-832.
- [7] M. Costa, *Annu. Rev. Pharmacool. Toxicol.*, **1991**, *31*, 321-337.
- [8] K.S. Kasprzak, *Chem. Res. Toxicol.*, **1991**, *4*, 604-615.
- [9] X.P. Jin, L. Zhang, H.Q. Gao, J.H. Fang, R.F. Li, *Prog. Chem.*, **2013**, *25*, 1898-1905.
- [10] J.J. Martinez Medina, M.S. Islas, L.L. Lopez Tevez, E.G.Ferrer, N.B. Okulik, *J. Mol. Struct.*, **2014**, *1058*, 298-307.

- [11] S. Anbu, S. Killivalavan, E.C.B.A. Alegria, G. Mathan, M. Kandaswamy, *J. Coord. Chem.*, **2013**, *66*, 3989-4003.
- [12] R.O. Bonello, I. R. Morgan, B.R.Yeo, L.E.J. Jones, B.M. Kariuki, *J. Organomet. Chem.*, **2014**, *749*, 150-156.
- [13] M. Gomleksiz, C. Alkan, B.S. Erdem, *Afr. J. chem.*, **2013**, *66*, 107-112.
- [14] M. Eslami Moghadam, A. Divsalar, A. Abolhosseini, A. K.Saboury, *J. Biomol. Struct. Dyn.*, **2015**, Accepted.
- [15] J.K. Barton, A.T. Danishefsky, J.M. Goldberg, *J. Am. Chem. Soc.*, **1984**, *106*, 2172-2176.
- [16] R.F. Pasternack, E.J. Gibbs, J.J.Villafranca, *Biochem.*, **1983**, *22*, 2406-2414.
- [17] G. Pratviel, J. Bernadou, B.J. Meunier, *Adv. Inorg. Chem.*, **1998**, *45*, 251-312.
- [18] N. Shahabadi, Z. Mirzaei, N. Hosseinpour Moghadam, *Spectrochim Acta A Mol Biomol Spectrosc.*, **2012**, *96*, 723-728.
- [19] Y.N. Xiao, C.X. Zhan, *J. Appl. Polym. Sci.*, **2002**, *84*, 887-893.
- [20] A.M. Pyle, J.P. Rehmann, R. Meshoyrer, C.V. Kumar, N.J. Turro, J.K. Barton, *J. Am. Chem. Soc.*, **1989**, *111*, 3051-3058.
- [21] S. Das, G.S. Kumar, *J. Mol. Struct.*, **2008**, *872*, 56-63.
- [22] S.C. Bi, D. Qiao, D. Song, Y. Tian, D. Gao, Y. Sun, H. Zhan, *Sens. Actuators, B. Chem.*, **2006**, *119*, 199-208.
- [23] T.R. Li, Z. Yang, B. Wang, D.D. Qin, *Eur. J. Med. Chem.*, **2008**, *43*, 1688-1695.
- [24] N. Shahabadi, S. Kashanian, F. Darabi, *Eur. J. Med. Chem.*, **2010**, *45*, 4239-4245.
- [25] S. Sharma, S. Singh, K.M. Chandra, D.S. Pandey, *J. Inorg. Biochem.*, **2005**, *99*, 458-466.
- [26] J. Olmsted, D.R. Kearns, *Biochem.*, **1977**, *16*, 3647-3654.
- [27] Y. Ni, D. Lin, S. Kokot, *Anal. Biochem.*, **2006**, *352*, 231-242.
- [28] J. Zhao, W. Li, R. Ma, S. Chen, S. Ren, T. Jiang, *Int. J. Mol. Sci.*, **2013**, *14*, 16851-16865.
- [29] F.J. Meyer, D. Porschke, *Biochem.*, **1993**, *32*, 4246-4253.
- [30] M.R. Eftink, C. A. Ghiron, *Anal. Biochem.*, **1981**, *114*, 199-227.
- [31] Y.J. Jang, G.Y. Yeo, B. Park, S.K. Kim, *Biophys. Chem.*, **2011**, *158*, 38-45.
- [32] D.J. Tan, Y. He, L. Qiu, Z.T. Zhang, *Chem. Res. Appl.*, **2007**, *19*, 502-506.
- [33] S. Kashanian, M. M Khodaei, P. Pakravan, *DNA .Cell.*, **2010**, *29*, 639-646.
- [34] M. Cory, D.D. Mckee, J. Kagan, D.W. Henry, J. Miller, *J. Am. Chem. Soc.*, **1985**, *107*, 2528-2536.
- [35] M. Waring, *J. Mol. Biol.*, **1965**, *13*, 269-282.